

Supporting Information for:

Measuring Remodeling of the Lipid Environment Surrounding Membrane Proteins with Lipid Exchange and Native Mass Spectrometry

Guozhi Zhang^{1,‡}, James E. Keener^{1,‡}, Michael T. Marty^{1,2,*}

¹Department of Chemistry and Biochemistry and ²Bio5 Institute, University of Arizona, Tucson, AZ 85721.

*Email: mtmarty@email.arizona.edu

Table of Contents

| | |
|---|----|
| SUPPLEMENTAL METHODS | 2 |
| Protein Expression and Purification..... | 2 |
| Nanodisc Assembly and Purification..... | 2 |
| Native MS of AmtB Nanodiscs | 2 |
| Native MS Data Analysis..... | 3 |
| Lipid Exchange | 4 |
| Separation of Exchanged Nanodiscs..... | 4 |
| Mass Spectrometry Analysis of Lipid Exchange..... | 4 |
| Lipid Exchange Data Analysis..... | 5 |
| LX-MS Method Validation..... | 6 |
| SUPPLEMENTAL FIGURES..... | 7 |
| Figure S1 | 7 |
| Figure S2..... | 8 |
| Figure S3..... | 9 |
| Figure S4..... | 10 |
| Figure S5..... | 11 |
| SUPPLEMENTAL REFERENCES | 11 |

SUPPLEMENTAL METHODS

Protein Expression and Purification

HIS-MBP-TEV-AmtB and membrane scaffold protein MSP1E3D1 were expressed in *E. coli* and purified as previously described.^{1,2} Briefly, AmtB was purified by immobilized metal affinity chromatography (IMAC) followed by size exclusion chromatography (SEC) with a Superdex 200 16/600 (GE Healthcare) in 0.025% dodecylmaltoside (DDM, Anatrace) buffer. MSP1E3D1 was purified by IMAC using established protocols.³

Nanodisc Assembly and Purification

AmtB nanodiscs were assembled using MSP1E3D1(-) or added threonine variants¹ to accommodate the large AmtB trimer and prepared similar to as previously described.^{1,2,4} MSP1E3D1(-) is the cleaved version of MSP1E3D1 where the polyhistidine tag has been removed by TEV protease. 1-Palmitoyl-2-oleoyl-*sn*-glycero-3-phosphocholine (POPC) and 1-palmitoyl-2-oleoyl-*sn*-glycero-3-phospho-(1'-*rac*-glycerol) (POPG) lipids from Avanti Polar Lipids were dissolved in chloroform and quantified by phosphate analysis.³ Lipids were dried and resuspended in 100 mM sodium cholate (Sigma Aldrich) prior to being mixed to a 50/50 or 0/100 POPC/POPG ratio. Spectra of AmtB nanodiscs with 100/0 POPC/POPG were collected previously² and are described therein. The reconstitution mixture of purified AmtB in DDM, mixed lipids in cholate, and MSP were incubated on ice for approximately 1 hour before adding Amberlite XAD-2 beads (Sigma Aldrich) for overnight detergent removal and nanodisc self-assembly at 4 °C. Empty nanodiscs were removed by IMAC, and membrane protein nanodiscs were further purified by SEC. Following overnight cleavage of the HIS-MBP tag with TEV protease, AmtB nanodiscs were then purified through another round of IMAC and SEC to isolate monodisperse nanodiscs with cleaved AmtB. Here, 0.2 M ammonium acetate at pH 6.8 (Sigma Aldrich) was used as the mobile phase for SEC to exchange the AmtB nanodiscs into an MS-compatible buffer. The purity of AmtB nanodiscs was confirmed by SEC, and chromatograms agreed with prior experimental results.² Samples were concentrated to 1–5 μM and flash frozen at -80°C for storage. Because the polyhistidine tag was removed from both AmtB and MSP1E3D1(-), there was no polyhistidine tag on the AmtB nanodiscs.

Empty nanodiscs without membrane proteins were assembled and purified in a similar manner, as previously described.⁵ Here, either the polyhistidine-tagged MSP1E3D1 or the untagged MSP1E3D1(-) was used. Lipid stocks of POPC and POPG were prepared in cholate and mixed to the desired ratio prior to assembly.

For both lipid exchange and native MS, error bars are shown as the standard deviation of single measurements on three replicate nanodisc assemblies that were prepared and measured separately.

Native MS of AmtB Nanodiscs

Neat glycerol carbonate at >90% purity (Tokyo Chemical Industry Co., Inc.) or propylene carbonate at 99.5% purity (Arcos Organics) were mixed 1:19 v/v with AmtB nanodiscs prior to native MS to create a 5% solution of supercharging reagent. Nanodisc samples were gently mixed into the supercharging reagent at room temperature, and analysis by native MS was started within several minutes after mixing.

Native mass spectrometry was performed using an Ultra-High Mass Range (UHMR) Q-Exactive HF quadrupole-Orbitrap mass spectrometer⁶ as previously described.² Nano-electrospray ionization (nESI) was performed with capillary needles prepared using a P-1000 micropipette puller (Sutter Instrument, Novato, CA). Instrumental settings were used as previously stated.^{1,2,7} Key instrument settings included 1.1–1.5 kV for capillary voltage and 200 °C for capillary temperature. Scans were collected from 2,000–30,000 m/z with 10 microscans summed into one scan at a resolution setting of 15,000. The collision voltage was applied in the HCD cell and increased from 0 to 200 V in 20 V increments at 1-minute acquisitions for each step.

Native MS Data Analysis

Native MS data analysis of AmtB nanodiscs was performed using UniDec and MetaUniDec.^{7,8} The lower mass limit was set to 29 kDa. The upper mass limits were set to 200, 250, or 350 kDa depending on the species present in each spectrum, and limits were only set after examining broader mass ranges. For data with upper mass limits of 200/250 and 350 kDa, the charge ranges were 1–25 and 1–35, respectively. The mass was sampled every 1 Da, and the peak full width at half max (FWHM) was set to 2.5 Th for samples with glycerol carbonate and 10 Th otherwise, using a Gaussian peak shape function. Mass differences were set to 760 Da and 754.5 Da for 100% POPC and 50/50 POPC/POPG nanodiscs, respectively. Finally, the charge smooth width, point smooth width, and mass smooth width were all set to 1.

To determine the average mass of lipids bound to AmtB, we first extracted the center of mass for each peak from the zero-charge mass distribution, using the intensities above 50% of the maximum intensity for that peak to avoid distortions from noise or baseline. We then subtracted the mass of the protein components, either AmtB alone in the case of glycerol carbonate or no additive spectra (where AmtB was ejected from the nanodisc), or AmtB with two MSP belts for propylene carbonate (where AmtB was retained in a largely intact nanodisc). To correct for small differences in adduction or errors in mass accuracy, the mass of the protein components was corrected by using a linear regression of the number of bound lipids versus the center of mass. Here, the y-intercept corresponded to the corrected mass of the protein components without lipids. The average correction was typically around 10–20 Da, around the mass of one water or ammonium molecule. This correction was only necessary and only applied for glycerol carbonate spectra because small mass errors are divided out when more lipids are bound (see below), which is the case with no additive and propylene carbonate. For each peak, subtracting the mass of the protein components gave the total mass of the lipids, which we then divided by the number of lipids present in the complex to get the average lipid mass for each peak. Because not all peaks were present at all collision voltages, these operations were performed for each peak on each separate collision voltage over a specified range, and the overall average mass for each peak was taken as the average from each collision voltage step weighted by its squared intensity at that voltage.

The first two peaks, for 1 and 2 bound lipids, showed large error bars for control samples with only POPC lipids, so they were discarded. This is likely because subtle shifts or errors in the mass are divided out at higher numbers of lipids. For example, a 5 Da (around 40 ppm) shift in the mass would cause an apparent absolute shift of 45% in the mole percentage of POPC for the first lipid because the difference in mass between POPC and POPG is 11 Da. However, the same shift divided over two lipids would only lead to a 23% shift in the mole percentage. Over three lipids,

it would give a 15% shift, and so on following a $1/n$ decay. Thus, the average mass values become much more accurate with higher numbers of lipids bound.

Lipid Exchange

AmtB nanodiscs with a 50% POPC mole percentage, defined as $100 \times \text{POPC}/(\text{POPC}+\text{POPG})$, were mixed with empty polyhistidine-tagged MSP1E3D1 nanodiscs with POPC mole percentages of 0, 20, 40, 60, 80, or 100% at a 1:1 molar ratio and a final concentration of 2.3 μM AmtB nanodiscs. To extend the titration to a lower total POPC mole percentage (X_t), the AmtB nanodiscs were mixed with 0% POPC empty nanodiscs at a 1:2.6 molar ratio while keeping the AmtB nanodiscs at 2.3 μM . The mixtures were incubated at room temperature (21–23 °C) for 2.8 days to allow the lipid exchange to reach equilibrium. All experiments were performed in 0.2 M ammonium acetate solution at pH 6.8. Preliminary experiments showed that exchanges at longer time points were within experimental error of exchanges at 2.8 days, demonstrating that the solution approached equilibrium by 2.8 days. A slight systemic deviation was observed (Figure S1), suggesting that it may not have fully reached equilibrium, but it was within the precision of the measurement. Although we used different lipids, these time scales were roughly consistent with prior experiments.⁹ Control experiments were also performed using 50% POPC untagged empty nanodiscs mixed with empty polyhistidine-tagged MSP1E3D1 nanodiscs in mole percentages of 0, 20, 40, 60, 80, or 100% at a 1:1 molar ratio and a 2.3 μM final concentration of each nanodisc as well as at a 1:2.6 molar ratio with 0% POPC nanodiscs.

Separation of Exchanged Nanodiscs

After exchanging, tagged empty nanodiscs and untagged (either empty or AmtB) nanodiscs were separated by IMAC using a Ni-NTA His SpinTrap (GE Healthcare). Because small exchange volumes of roughly 16 μL were used, around 1/3 of the 100 μL column volume was removed for a final column volume around 66 μL . The SpinTrap was prepared by three washes of 450 μL loading buffer (20 mM imidazole, 0.2 M ammonium acetate, pH 7.6) to equilibrate the column. Prior to addition to the beads, the imidazole concentration of the exchange mixture was adjusted to 20 mM by adding a 1 M imidazole solution (pH 7.6 adjusted with acetic acid) to limit the non-specific binding of the untagged nanodiscs. Then, the exchange reaction mixture was added to the IMAC beads and allowed to incubate for 1–2 minutes at 4 °C. The flow-through was removed by centrifugation at 100 g for 45 seconds, and extra loading buffer of 20 μL was added to the column and washed under the same centrifugation procedures. Preliminary tests with only untagged nanodiscs showed that the concentration of nanodiscs was highest in the first wash due to the small volumes of sample used. Thus, the first wash was collected for MS analysis to maximize the lipid concentration. Around 20 μL was typically recovered. After separation, the His SpinTrap was cleaned with three washes of 450 μL elution buffer (400 mM imidazole, 0.2 M ammonium acetate, pH 7.8). The tagged empty nanodiscs were not recovered nor analyzed. We did not attempt to collect the eluted tagged nanodiscs to simplify the experiment, avoid sample cleanup to remove the 0.4 M imidazole, and so that nonspecific binding of untagged nanodiscs was not a concern.

Mass Spectrometry Analysis of Lipid Exchange

Because PC and PG lipids ionize best in positive and negative mode, respectively, measurements were made in both ionization modes through separate injections. Lipid ionization efficiency is dominated by the head groups,¹⁰ so we used lipids with the same head groups but different tail

lengths as internal standards: 1,2-dimyristoyl-*sn*-glycero-3-phosphocholine (DMPC) and 1,2-dimyristoyl-*sn*-glycero-3-phospho-(1'-*rac*-glycerol) (DMPG). Internal standards were dissolved separately in chloroform, and their concentrations were measured by phosphate analysis (see above). Immediately after quantification, both standards were mixed to a 1:1 molar ratio in a glass tube, dried together, and resuspended in methanol to a final concentration around 2.6 mM. This stock solution of internal standards was then diluted 30–50 fold before addition to nanodisc samples.

Prior to analysis, nanodisc samples after IMAC separation (untagged only) were mixed with 10 μL of diluted internal standard to a final volume around 30 μL . Nanodisc samples without IMAC separation (tagged and untagged) were more concentrated and thus were mixed with 20 μL of internal standard to a final volume around 25 μL . The sample was briefly vortexed to ensure complete mixing of the internal standard. An Agilent 1260 Infinity II HPLC system was used to perform the direct flow injection of 5 μL of samples to the MS. Each flow injection was 3 minutes at a flow rate of 80 $\mu\text{L}/\text{min}$. No LC was required because the lipid mixtures were very simple, and the exchange was performed in MS-compatible ammonium acetate buffer. Positive ionization mode was used to analyze PC lipids using a 90% methanol with 0.1% formic acid solvent. Negative ionization mode was used to analyze PG lipids using 90% methanol with 0.1% ammonium hydroxide. The injection needle was washed with 5% acetonitrile after each injection, and two blanks of methanol were injected between each sample injection to ensure no carryover of the previous sample.

Mass spectrometry was performed using a Waters Micromass Quattro Micro triple quadrupole mass spectrometer with an ESI source. Key tune parameters were:

Positive Mode: 3.3 kV capillary voltage, 35 V cone voltage, 4 V extractor voltage, 100 °C source temperature, 150 °C desolvation temperature, and the desolvation gas flow at 105.8 L/hr.

Negative Mode: -3.3 kV capillary voltage, -30 V cone voltage, -3 V extractor voltage, 100 °C source temperature, 150 °C desolvation temperature, and the desolvation gas flow at 250 L/hr.

For positive mode, full scans were collected over a mass range of 100–1000 m/z using a 1 second scan time and 0.1 second inter-scan delay. The monoisotopic peak of both POPC and DMPC were integrated to get the signal intensity from each.

For negative mode, selected ion monitoring was used because the negative mode signal was generally lower. Here, a 0.25 second dwell time was used at the monoisotopic m/z of POPG and DMPG with a 0 span, 0.02s inter-channel delay, and 0.02 second inter-scan delay.

Lipid Exchange Data Analysis

To quantify the relative mole percentages of POPC and POPG, the intensities measured by MS (I_{POPC} and I_{POPG}) were normalized by dividing by the intensities of the internal standards, DMPC and DMPG (I_{DMPC} and I_{DMPG}), respectively. Because internal standards were prepared in a 1:1 molar ratio of DMPC:DMPG, the normalized signals could then be compared directly. Thus, the

relative mole percentage, X , of POPC was calculated as: $100 \times \frac{\frac{I_{POPC}}{I_{DMPC}}}{\frac{I_{POPC}}{I_{DMPC}} + \frac{I_{POPG}}{I_{DMPG}}}$. We refer to the total

POPC mole percentage as X_t , the mole percentage in the membrane protein nanodiscs alone as X_p , and the mole percentage in empty but untagged nanodiscs as X_u .

To determine the isolipid point, the plot of X_t versus $X_p - X_t$ was fit to a sigmoidal curve of the form: $y = a + \frac{b}{1+e^{-c(x-d)}}$ in Python using the SciPy library. The fit was global across all three replicates. The equation with fit parameters was then solved to determine the X_t value (x) where $y = X_p - X_t = 0$, the isolipid point. The uncertainty of the isolipid point was determined with bootstrapping using random sampling with replacement. Fits to different order polynomials yielded similar isolipid points.

LX-MS Method Validation

To validate that the internal standards had similar ionization efficiencies to the analyte lipids, we created known mixtures of DMPC/POPC or DMPG/POPG in methanol with a broad range of ratios from 0.2:1 to 20:1. The measured ratios of $\frac{I_{POPC}}{I_{DMPC}}$ or $\frac{I_{POPG}}{I_{DMPG}}$ versus their expected values both showed a linear response with slopes close to 1.

To validate that the mole percentage of POPC was accurate, three known mixtures of POPC and POPG in methanol were prepared with different POPC mole percentages (25, 50, and 75%). These three known mixtures were analyzed daily as described above to confirm the measurement accuracy. The absolute standard deviations of the measurements were all around 2–5% POPC and were less than one standard deviation from the known mole percentage.

The method was also validated with nanodiscs prepared at known lipid compositions. Untagged empty nanodiscs prepared with 0, 25, 50, 75, and 100% POPC and AmtB nanodiscs with 50% POPC were measured as described above. Similar to known lipid mixtures in methanol, nanodiscs showed an absolute measurement standard deviation around 2–5% POPC and were generally within one standard deviation of the known mixture.

To validate the IMAC separation, the untagged nanodiscs with known ratios (0, 25, 50, 75, and 100%) were added to the IMAC beads and then collected as described. The same analysis was also performed for the 50% POPC AmtB nanodiscs to verify that there was no significant change in lipid mole percentage due to the separation. The capture of tagged empty nanodiscs was validated by performing the same separation and analysis procedure on tagged nanodiscs alone. Here, no quantifiable amount of POPC or POPG was detected, confirming that the contribution of uncaptured tagged nanodiscs is negligible.

Finally, we also tested whether flipping the starting lipid composition would influence the final distribution. Here, duplicate assemblies of AmtB nanodiscs were prepared with 0% POPC (100% POPG) and were exchanged with 50% tagged empty nanodiscs. The X_t values were higher than the mixture of 50% AmtB nanodiscs with 0% empty nanodiscs because AmtB displaces lipids from the nanodisc, leading to more POPC in the total lipid pool for the flipped experiment. Nevertheless, the results were consistent with the curve in Figure 1, demonstrating that the equilibrium $X_p - X_t$ differences were independent of the starting lipid composition.

SUPPLEMENTAL FIGURES

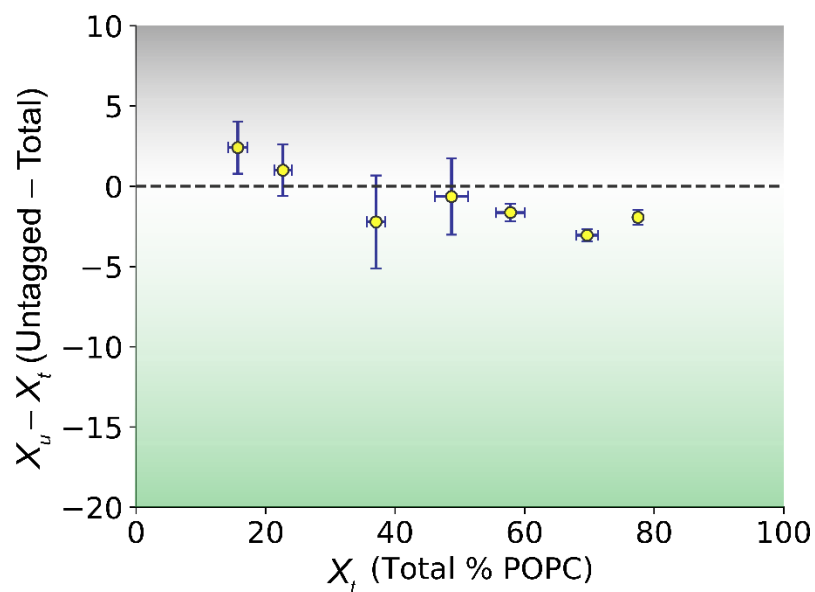


Figure S1. Lipid exchange of untagged 50/50 POPC/POPG empty nanodiscs mixed with tagged empty nanodiscs at different initial POPC/POPG ratios. The total mole percentage of POPC in the mixture of tagged and untagged nanodiscs (X_t) is shown on the x-axis with the difference in mole percentage of POPC between the untagged nanodiscs alone (X_u) and the total mixture ($X_u - X_t$) on the y-axis.

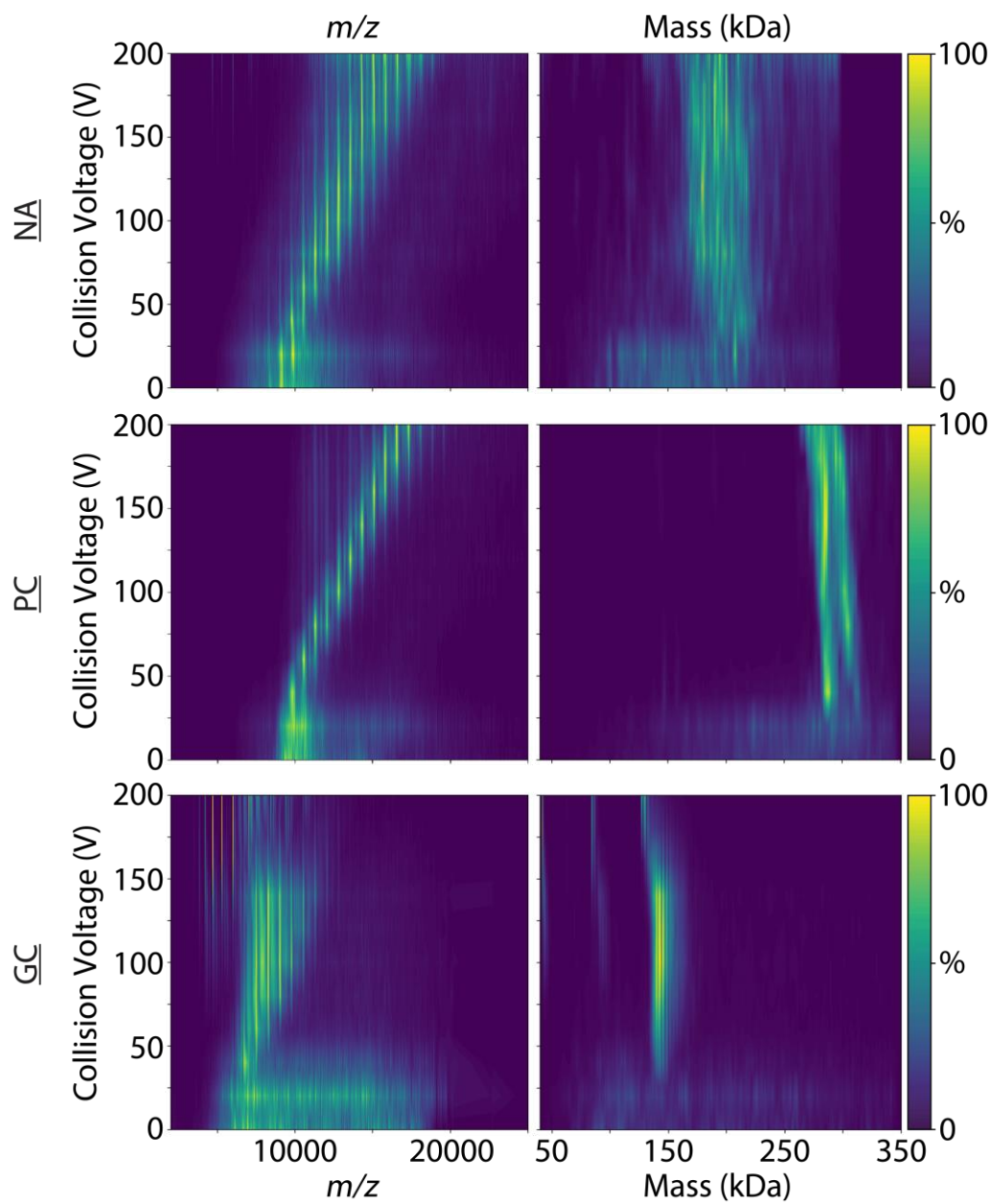


Figure S2. Representative mass spectra (*left*) and deconvolved mass distributions (*right*) of 50/50 POPC/POPG AmtB nanodiscs with no additive (NA, *top*), propylene carbonate (PC, *middle*), and glycerol carbonate (GC, *bottom*) from 0–200 V.

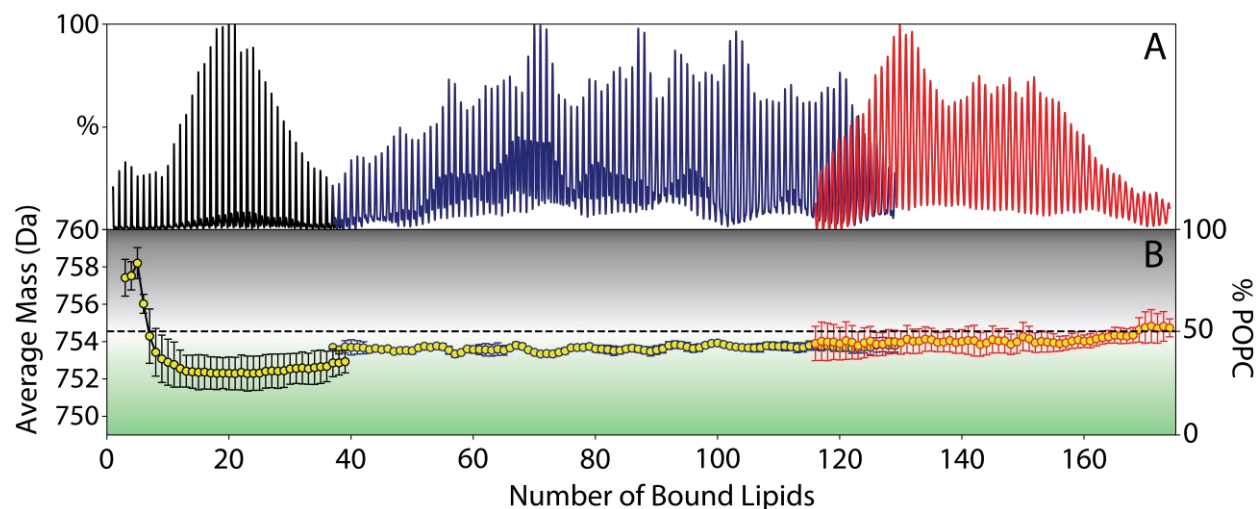


Figure S3. A) Summed deconvolved mass spectra of 50/50 POPC/POPG nanodiscs with embedded AmtB. Spectra were collected with added glycerol carbonate (*black*), no additive (*blue*), and propylene carbonate (*red*). B) The average mass of bound lipids for each peak (*left axis*) along with the relative mole percentage of POPC (*right axis*). A separate peak series is observed in no additive spectra that is potentially a small amount of contaminant lipid or detergent. The expected average lipid mass of 754.5 Da for 50/50 POPC/POPG is indicated by a dashed line. Spectra are summed from 60–200 V except no additive, which is from 60–120 V.

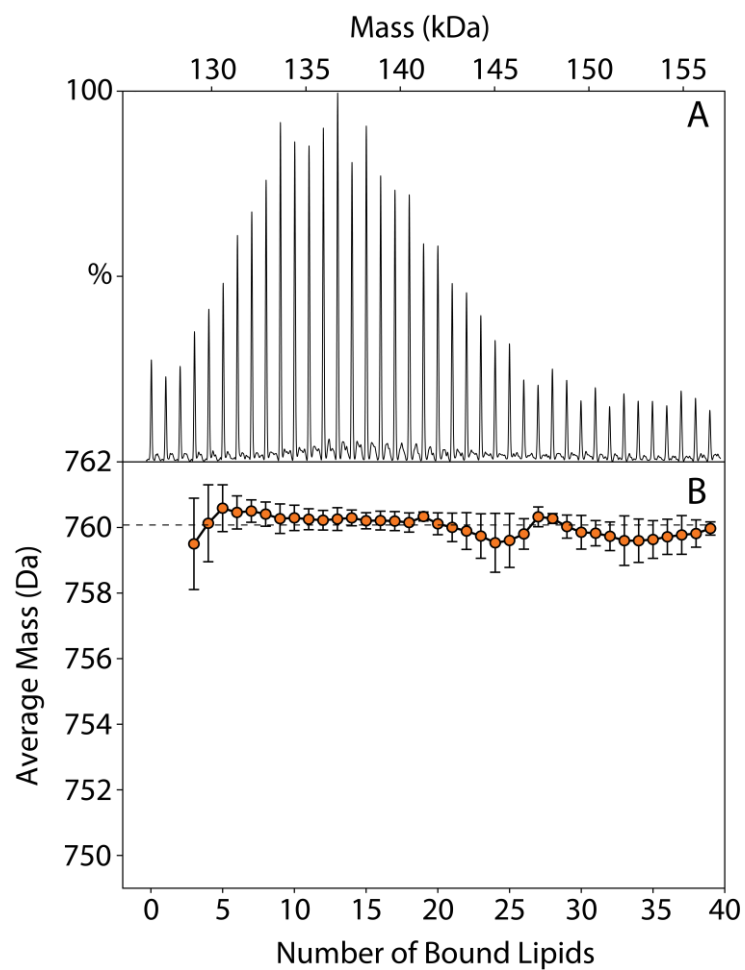


Figure S4. A) Summed deconvolved mass spectrum (60–300 V) of AmtB trimer ejected from 100% POPC nanodiscs. B) The average mass of bound lipids (60–300 V) shows the expected average lipid mass of 760 Da (indicated by a dashed line) for pure POPC.

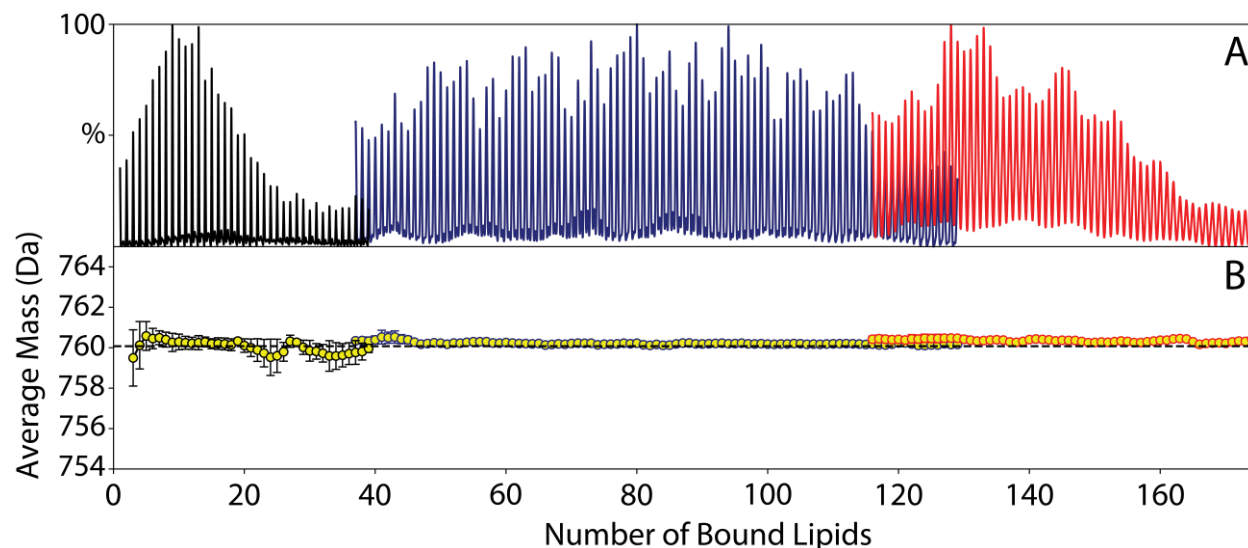


Figure S5. A) Summed deconvolved mass spectra of 100% POPC nanodiscs with embedded AmtB. Complexes were activated in the presence of glycerol carbonate (*black*), no additive (*blue*), and propylene carbonate (*red*). B) The average mass of bound lipids shows that nanodiscs have the expected average lipid mass of 760 Da (indicated by a dashed line) for pure POPC for all mass regimes. Spectra are summed from 60–300 V except no additive, which is from 60–120 V.

SUPPLEMENTAL REFERENCES

- (1) Reid, D. J.; Keener, J. E.; Wheeler, A. P.; Zambrano, D. E.; Diesing, J. M.; Reinhardt-Szyba, M.; Makarov, A.; Marty, M. T. Engineering Nanodisc Scaffold Proteins for Native Mass Spectrometry. *Anal. Chem.* **2017**, *89*, 11189-11192.
- (2) Keener, J. E.; Zambrano, D. E.; Zhang, G.; Zak, C. K.; Reid, D. J.; Deodhar, B. S.; Pemberton, J. E.; Prell, J. S.; Marty, M. T. Chemical additives enable native mass spectrometry measurement of membrane protein oligomeric state within intact nanodiscs. *J. Am. Chem. Soc.* **2019**, *141*, 1054-1061.
- (3) Ritchie, T. K.; Grinkova, Y. V.; Bayburt, T. H.; Denisov, I. G.; Zolnerciks, J. K.; Atkins, W. M.; Sligar, S. G.: Reconstitution of Membrane Proteins in Phospholipid Bilayer Nanodiscs. In *Methods Enzymol.*; Nejat, D., Ed.; Academic Press: San Diego, CA, 2009; Vol. 464; pp 211-231.
- (4) Marty, M. T.; Hoi, K. K.; Gault, J.; Robinson, C. V. Probing the Lipid Annular Belt by Gas-Phase Dissociation of Membrane Proteins in Nanodiscs. *Angew. Chem. Int. Ed. Engl.* **2016**, *55*, 550-554.
- (5) Hoi, K. K.; Robinson, C. V.; Marty, M. T. Unraveling the Composition and Behavior of Heterogeneous Lipid Nanodiscs by Mass Spectrometry. *Anal. Chem.* **2016**, *88*, 6199-6204.
- (6) van de Waterbeemd, M.; Fort, K. L.; Boll, D.; Reinhardt-Szyba, M.; Routh, A.; Makarov, A.; Heck, A. J. High-fidelity mass analysis unveils heterogeneity in intact ribosomal particles. *Nat. Methods* **2017**, *14*, 283-286.

- (7) Reid, D. J.; Diesing, J. M.; Miller, M. A.; Perry, S. M.; Wales, J. A.; Montfort, W. R.; Marty, M. T. MetaUniDec: High-Throughput Deconvolution of Native Mass Spectra. *J. Am. Soc. Mass Spectrom.* **2019**, *30*, 118-127.
- (8) Marty, M. T.; Baldwin, A. J.; Marklund, E. G.; Hochberg, G. K.; Benesch, J. L.; Robinson, C. V. Bayesian deconvolution of mass and ion mobility spectra: from binary interactions to polydisperse ensembles. *Anal. Chem.* **2015**, *87*, 4370-4376.
- (9) Cuevas Arenas, R.; Danielczak, B.; Martel, A.; Porcar, L.; Breyton, C.; Ebel, C.; Keller, S. Fast Collisional Lipid Transfer Among Polymer-Bounded Nanodiscs. *Sci. Rep.* **2017**, *7*, 45875.
- (10) Yang, K.; Han, X. Accurate quantification of lipid species by electrospray ionization mass spectrometry - Meet a key challenge in lipidomics. *Metabolites* **2011**, *1*, 21-40.